Chinese Herbal Medicines 13 (2021) 105–115

Contents lists available at ScienceDirect

Chinese Herbal Medicines

journal homepage: www.elsevier.com/locate/chmed

Original Article

Neuroprotective effects of kukoamine A on 6-OHDA-induced Parkinson's model through apoptosis and iron accumulation inhibition

Xin Li [a], Xiao-wen Jiang [a,c], Hai-xiao Chu [a], Qing-chun Zhao [a,*], Huai-wei Ding [b,*], Chao-hong Cai [a,*]

[a] Department of Pharmacy, General Hospital of Northern Theater Command, Shenyang 110840, China
[b] Key Laboratory of Structure-Based Drug Design and Discovery, Ministry of Education, Shenyang Pharmaceutical University, Shenyang 110016, China
[c] Department of Traditional Chinese Medicine, Shenyang Pharmaceutical University, Shenyang 110016, China

ARTICLE INFO

Article history:
Received 5 January 2020
Revised 6 April 2020
Accepted 16 April 2020
Available online 8 December 2020

Keywords:
6-OHDA
iron chelation
iron homeostasis
kukoamine A
neuroprotection
Parkinson's disease

ABSTRACT

Objective: Parkinson's disease (PD) is characterized by the loss of dopaminergic neurons in substantia nigra (SN). Our previous study demonstrated kukoamine A (KuA) to exhibit strong neuroprotective effects through antioxidative stress, and autophagy in MPTP/MPP$^+$-induced PD models *in vivo* and *in vitro*. It is necessary to evaluate the efficacy of the anti-PD effects under various models.
Methods: In the present study, total chemical synthesis was used to obtain KuA, which performed low content in *Lycii Cortex*. Then, 6-OHDA-induced PD model of PC12 cells was used to investigate the effects of KuA on PD.
Results: Our results demonstrated that KuA ameliorated cell loss and mitochondrial membrane potential (MMP) loss, and inhibited Bax/Bcl-2 ratio increase that were induced by 6-OHDA. Iron accumulation in SN is thought to participate in neuronal death in PD, which subsequently resulted in oxidative stress and overexpression of α-synuclein caused by iron metabolism protein disorder. In our study, KuA could chelate cellular iron content and decrease iron influx. Moreover, KuA could upregulate the expression of ferroportin1 and Hephaestin, downregulate the expression of DMT1, TfR, and Ferritin to maintain cellular iron homeostasis avoiding neuronal death from cellular iron deposition. Moreover, KuA could decrease the expression of a-synuclein in cells. All the results indicated that KuA protected against neurotoxin-induced PD due to the apoptosis inhibition and iron homeostasis maintaining.
Conclusion: KuA treatment might represent a neuroprotective treatment for PD.

1. Introduction

Parkinson's disease (PD) is associated with the degeneration of dopaminergic neurons in the substantia nigra pars compacta (SNpc). One of the pathological hallmarks of PD is the presence of intracellular inclusions called Lewy bodies that consist of aggregates of the presynaptic soluble protein called a-synuclein (Jomova et al., 2010). Clinical manifestations of PD include motor impairments involving resting tremor, a slowing of physical movement (bradykinesia), postural instability, gait difficulty, and rigidity and non-motor impairments including cognitive deficits, emotional changes, sleep and sensation disturbances and autonomic dysfunction (Afshin-Majd et al., 2017). Although the exact mechanisms underlying PD are largely unknown, extensive evidences show that selective high levels of iron, and oxidative stress, mitochondrial dysfunction, and abnormal protein aggregation resulted from iron accumulation in the SNpc contribute to the pathogenesis of PD (Xu et al., 2010; Jung et al., 2017), leading to the dopaminergic neuronal loss.

Iron is a highly redox-reactive metal, which is needed for numerous catalytic and metabolic processes including as a cofactor for tyrosine hydroxylase (TH), a biomarker of normal neuronal function, and disturbance of intracellular Fe homeostasis results in impairment of critical functions in biological systems and neurological disorders, including Parkinson's disease and Alzheimer's disease (Zhou et al., 2014). There is consistent evidence of a regional increase of iron in the SNpc of PD patients as well as rapid accumulation of nigral iron in animals following intoxication with the Parkinsonian agents 6-hydroxydopamine (6-OHDA) and 1-methy l-4-phenyl-1,2,3,6-tetrahydropyridine (MPTP) (Finkelstein et al., 2017). Many proteins are involved in cellular Fe influx, Fe efflux as well as storage to maintain Fe homeostasis. Iron could be transported into mammalian cells via the transferrin (Tf)-Tf receptor (TfR) and non-transferrin-bound iron (NTBI) pathways. Divalent

* Corresponding authors.
E-mail addresses: Zhaoqingchun1967@163.com (Q.-c. Zhao), dinghuaiwei627@163.com (H.-w. Ding), cch9970@163.com (C.-h. Cai).

https://doi.org/10.1016/j.chmed.2020.12.004
1674-6384/

metal transporter 1 (DMT1) is one of the iron transporters involved in NTBI pathway (Xu et al., 2010), and increased DMT1 expression was found in the SN of PD model, such as 6-OHDA. Ferroportin1, also known as SLC11A3, is a multiple transmembrane domain protein identified in several cell types involved in the export of cellular iron, and evidence has indicated that iron exit is dependent only on ferroportin1 (Zhou et al., 2014). Due to the suggested involvement of iron trafficking proteins and iron accumulation in PD, some compounds that could regulate iron transporting proteins and then /or directly alleviate iron deposition might have pharmaceutical value in the treatment of PD, which supported by the case of the high affinity iron chelator deferiprone being reported to provide benefit in a phase 2 randomized clinical trial in PD patients (Devos et al., 2014).

Lycii Cortex, a traditional Chinese herb, was generally used as a tonic and reported to exhibit hypotensive, hypoglycemic, antipyretic and anti-stress ulcer activity in animal experiment (Funayama et al., 1980). Kukoamine A (KuA) is a major bioactive component in *Lycii Cortex* and the chemical structure was shown in Fig. 1, whose content just <0.1% in *Lycii Cortex*. Our previous study showed that KuA could block the oxidative-stress and excitotoxicity induced by NMDA (Hu et al., 2015), and could also attenuate the brain damage and neuroinflammation induced by radiation and pMCAO (Zhang et al., 2016a, 2016b, 2016c; Liu et al., 2017). Furthermore, we found that KuA showed the anti-PD activity against MPTP/MPP^+ *in vivo* and *in vitro* through activation of autophagy (Hu et al., 2017). However, whether KuA showed the same effects on other more PD models are still unknown.

Neuroblastoma PC12 cells treated with 6-OHDA are widely used as a valuable cell model of dopaminergic neuronal cell death to mimic the pathophysiologic degeneration. In this study, we firstly synthesized KuA on the basis of previous studies (Piletska, Burns, Terry, & Piletsky, 2012; Vassis et al., 2001), and then evaluated the effect of KuA on PC12 cells *in vitro*. To find the mechanism inside protective effect of KuA, expressions of mediators involved in the mitochondrion-mediated apoptotic pathway and MAPK pathway were investigated in this research. In addition, KuA alone was used to testify its iron chelation, and the decrease of iron accumulation and regulation of iron regulatory protein. All the results indicated that KuA may be a promising agent for PD treatment.

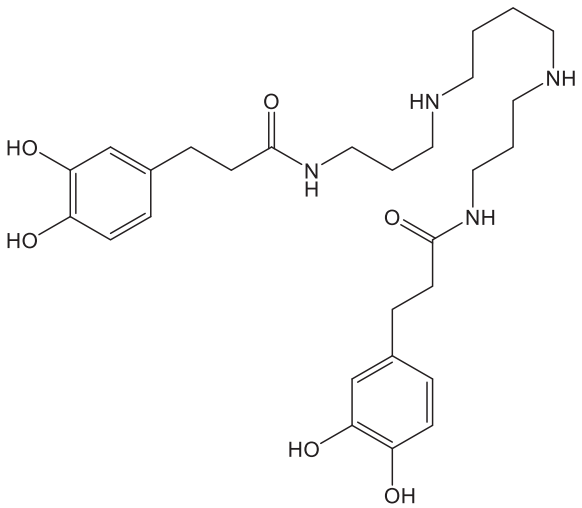

Fig. 1. Structure of kukoamine A.

2. Materials and methods

2.1. Materials

3,4-Dihydroxyhydrocinnamic acid was purchased from HEOWNS (China, Tianjin). Spermine (SPM) was purchased from Aladdin (China, Shanghai). MTT, 6-hydroxydopamine hydrochloride (6-OHDA) was purchased from Sigma-Aldrich (St. Louis, MO, USA). Calcein AM was purchased from Abcam (Cambridge, UK). Deferoxamine mesylate (>98%) was purchased from MedChemexpress (New Jersey, USA). LDH Cytotoxicity Assay Kit, Annexin V-FITC Apoptosis Detection Kit, Reactive Oxygen Species Assay Kit, Lipid Peroxidation MDA Assay Kit, Total Superoxide Dismutase Assay Kit with WST-8, JC-1staining Kit were purchased from Beyotime (Nanjing, China). Hoechst 33,342 was purchased from Invitrogen (Carlsbad, CA, USA). Rabbit antibodies to Bcl-2, Bax, cytochrome *C*, Transferrin Receptor, Ferritin were purchased from Abcam (Cambridge, UK). Tyrosine hydroxylase (TH) and α-synuclein were purchased from Cell Signaling Technology (Beverly, MA, USA). Caspase-3, Caspase-9, PARP were purchased from Wanleibio. (China, Beijing). Ferroportin1 was purchased from Novus Biologicals (SanDiego, California, USA). β-Actin, α-tublin, hephaestin, DMT1 and HRP-conjugated goat anti-rabbit (mouse) IgG were purchased from Proteintech. (Rosemont, USA). Other chemicals and regents available were purchased form local commercial sources. PC12 cell line was gifted by professor Lu Ke at China Medical University.

2.2. Synthesis of KuA

Using 3, 4-dihydroxyhydrocinnamic acid and spermine as raw materials, the synthetic route in the literatures (Piletska, Burns, Terry, & Piletsky, 2012; Vassis et al., 2001) was improved, then a yellow amorphous solid precipitated had gained. The synthesized KuA was dissolved in deuterated DMSO and analyzed using a Bruker ARX-300 NMR spectrometer (Bruker, Germany) operating at 400 MHz. The purity was detected by LC-16 (SHIMADZU, Japan), suggesting more than 98% (supplement figure).

2.3. Cell culture

The PC12 cell line was cultured in DMEM/F12 medium with 5% FBS and 5% Horse Serum (Gibco, USA) at 37 °C in a humidified (5% CO_2) incubator. Cells were seeded in different kinds of plates at different proper density and continued to culture for 24 h. KuA, 6-OHDA and deferoxamine mesylate (DFO) were respectively dissolved in DMSO, 9% NaCl with 0.2% vitamin C and ddH_2O as a concentrated stock and further diluted to their final concentration. Then, the stock solution of 6-OHDA and DFO were stored at −20 °C.

2.4. Cell viability assay

The cell viability was determined by the MTT assay. PC12 cells were seeded in 96-well plates (7×10^3 cells/well) and cultured for 24 h. Then the cells were treated with different concentration (0, 25, 50, 100 μmol/L) of 6-OHDA for 6, 8, 12 or 24 h to confirm the proper condition of cell injury. After that, cells were pretreated with KuA (5, 10, 20 μmol/L) or vehicle for 4 h and exposed to 6-OHDA. After incubation, cells in per well were added with MTT (final concentration: 0.5 mg/mL) and incubated for 4 h, then discarded them, and the formazan crystals were lysed with DMSO. The absorbance was detected at 490 nm. Cell viability was expressed as a percentage of control.

2.5. Lactate dehydrogenase (LDH) release assay

The cells were incubated as mentioned above. Then the LDH level was measured according to the manufacturer's instructions. The absorbance at 490 nm was measured by a microplate reader (Elx 800 Bio-Tek, USA).

2.6. Hoechst 33342 staining

A fluorescent DNA-binding dye, Hoechst 33342, was used to measure apoptosis (Zhang et al., 2016a, 2016b, 2016c). Cells were seeded in 6-well plates (20×10^4 cells/well) and treated as mentioned above. The nuclei were stained with Hoechst 33,342 (10 μmol/L) for 15 min at 37 °C in the dark. Images were obtained using a fluorescence microscope (IX71, Olympus, Japan).

2.7. Annexin V and PI double staining

Apoptosis rate was measured by flow cytometric analysis according to the protocol provided by the Annexin V-FITC apoptosis detection kit. Briefly, cells were treated as mentioned above, and then, were harvested and washed three times with cold PBS. The cells were centrifuged at 1000 g/min for 5 min, the supernatant was discarded and the pellet was resuspended in 195 μL binding buffer at a density of 1×10^5 cells, loaded with 5 μL Annexin V-FITC and 10 μL PI for 20 min at room temperature in the dark and detected by flow cytometer (Becton Dickinson, NJ, USA).

2.8. Detection of mitochondral membrane potential (MMP)

The MMP was measured using the fluorescent dye, JC-1. JC-1 can penetrate cells and healthy mitochondria. At low membrane potentials (apoptotic cells), JC-1 exists as a monomer which emits green fluorescence, which maximum emission wavelength is 529 nm. JC-1 aggregates and emits red fluorescence at higher membrane potentials (normal cells), which maximum emission wavelength is 590 nm (Luo et al., 2017). Cells were seeded in 6-well plates (20×10^4 cells/well) and treated as mentioned above. The cells were incubated with JC-1 staining solution ($1 \times$) for 20 min at 37 °C in the dark. Afterward, the cells were washed with JC-1 staining buffer ($1 \times$) twice, and then were captured by inverted fluorescence microscopy (IX71, Olympus, Japan).

2.9. Intracellular reactive oxygen species (ROS) assay

The level of intracellular ROS was measured by fluorescence with 2′,7′-dichloroflurescein diacetate (DCF2-DA) (Zhang et al., 2016a, 2016b, 2016c). The dye DCFH2-DA can penetrate into cells and becomes hydrolyzed to non-fluorescent dichlorofluorescin (DCF). DCF then reacts with "ROS" to form the highly fluorescent dichlorofluorescein. The fluorescence intensity reflects the ROS generation inside cells. Cells were seeded in 6-well plates (20×10^4 cells/well) and treated as mentioned above. Then, cells were stained with DCH2-DA in serum-free medium (5 μmol/L) for 20 min at 37 °C in the dark. After incubation, the fluorescence from the DCF was analyzed using an inverted fluorescence microscopy (IX71, Olympus, Japan) at excitation and emission wavelengths of 488 nm and 525 nm.

2.10. SOD and MDA levels

The superoxide dismutase (SOD) and malondialdehyde (MDA) were measured according to the technical method of the detection kits. Protein concentration was determined by using BCA protein kits. The enzyme activities were then normalized to the corresponding protein concentration for each group, and expressed as the percentage of control.

2.11. Calcein loading of cells

Calcein AM is a non-fluorescent molecule which can permeate cell membrane. It has high stabilization not affected by the pH of the solution. In the living cells, calcein emits strong green fluorescence (excitation: 495 nm, emission: 515 nm) after the removement of AM group by the cytoplasm esterases. However, calcein is highly sensitive to metal ions and can be combined with intracellular iron to convert to non-fluorescent substances, leading to the quenching of fluorescence. The cell iron level can be estimated by the change of fluorescence intensity (Jia et al., 2015).

2.11.1. Iron chelation assay

Cells were seeded into 6-well plates (25×10^4 cells/well) and cultured for 24 h. Then the cells were pretreated with KuA (20 μmol/L) for 4 h, washed with cold PBS for three times, and then incubated with calcein AM (1 μmol/L) for 30 min at 37 °C in dark. After incubation, the cells were washed with PBS for three times, and then incubated with 100 μmol/L ferrous iron (ferrous sulfate in ascorbic acid solution, 1:44 M ratio) for 30 min. Finally, the cells were washed with cold PBS for three times, and incubated with DFO (50 μmol/L) for 30 min, and then washed with PBS for three times, and lastly resuspended in 1 mL PBS. The fluorescence intensity was measured by flow cytometer (BD FACSCalibur, USA).

2.11.2. Ferrous iron influx assay

Cells were seeded into 6-well plates (20×10^4 cells/well) and cultured for 24 h. Then the cells were incubated with 6-OHDA (10 μmol/L) for 24 h after pretreatment with KuA (20 μmol/L) for 4 h, washed with cold PBS for three times, and then incubated with calcein AM (1 μmol/L) for 30 min at 37 °C in dark. After incubation, the cells were washed with PBS for three times, and then incubated with 100 μmol/L ferrous iron for 30 min. And the cells were then washed with cold PBS for three times, and lastly resuspended in 1 mL PBS. The fluorescence intensity was measured by flow cytometer (BD FACSCalibur, USA).

2.11.3. Iron accumulation assay

Cells were seeded into 6-well plates (20×10^4 cells/well) and cultured for 24 h. Then the cells were incubated with 6-OHDA (10 μmol/L) for 24 h after pretreatment with KuA (20 μmol/L) for 4 h. And then the cells treated as above. The fluorescence intensity was measured by flow cytometer (BD FACSCalibur, USA).

2.12. Western blot assay

The potential mechanism of KuA on 6-OHDA were investigated by western blot assay, the method was the same as previously (Hu et al., 2015). The cells were cultured as above. Then the RIPA lysis buffer was used to crack the cells for collecting the cytosolic proteins, which concentration was determined by BCA assay kit. The samples containing 50 μg of protein from each treatment condition was separated by SDS/PAGE and transferred to PVDF membranes (Millipore Corporation). Total proteins were blocked with 5% non-fat milk or 5% BSA at room temperature for 2 h, and then incubated with individual primary antibodies (Bax, Bcl-2, cytochrome C, Bad, PARP, tyrosine hydroxylase, α-synuclein, and ferroportin at 1:1000; Caspase-3, Caspase-9, hephaestin at 1:500; DMT1 at 1:800; transferrin receptor at 1:5000; Ferritin at 1:1500) shaking overnight at 4 °C. After three times of washing with TBST buffer, the membranes were incubated with the anti-rabbit of anti-mouse IgG secondary antibody (1:12,000) in TBST for 1 h at room temperature, followed by three times of washing. At the end of each treatment the binding of antibody was detected with BeyoECL Plus. The results were expressed as the percentage of control, which was deemed to be 100%.

2.13. Statistical analysis

The data were expressed as means ± S.E.M. using the software of GraphPad Prism 7.0. Statistical significance was values and evaluated with one-way analysis of variance followed by a Tukey's HSD-post hoc test. Differences with $P < 0.05$ were considered as statistically significant.

3. Results

3.1. Effect of 6-OHDA on cell viability in PC12 cells

After PC12 cells being cultured for 24 h, they were treated by 25, 50, and 100 μmol/L 6-OHDA for 6, 8, 12, and 24 h, respectively. The cell viability was examined by MTT assay, as shown in Fig. 2A, which was shown in time- and dose-dependent manner. After treatment with 6-OHDA (25, 50, and 100 μmol/L) for 24 h, the cell viability was decreased to (59.84 ± 0.70) % (Fig. 2B). One-way ANOVA revealed a significant difference between groups ($P < 0.0001$). Therefore, 100 μmol/L 6-OHDA for 24 h was chosen for the following experiments.

3.2. Effects of KuA on 6-OHDA-induced PC12 cell injury

In order to investigate the effect of KuA on neuronal injury induced by 6-OHDA in PC12 cells, different concentrations of KuA were exposed to cells. The results showed that lower than 80 μmol/L of KuA had no significant cytotoxicity (Fig. 2C). As shown in Fig. 2D, pretreatment with KuA (5, 10, and 20 μmol/L) could significantly increase the cell viability to (76.91 ± 2.71)%, (83.56 ± 2.16)%, and (87.28 ± 2.03)%, respectively. Moreover, the cell morphology was also improved compared with 6-OHDA injury group (Fig. 2E). Furthermore, the results were supported by LDH release (Fig. 2F) that KuA (5, 10, and 20 μmol/L) respectively reduced the LDH release to (22.45 ± 0.22)%, (4.54 ± 2.58)%, (3.74 ± 1.52)% compared with 6-OHDA-treated group (40.33 ± 1.34)%. These results suggested that KuA had the protective effects on 6-OHDA-induced PC12 cells injury.

3.3. Effects of KuA on 6-OHDA-induced PC12 cell apoptosis

In order to investigate the anti-apoptotic effect of KuA on 6-OHDA-induced nerve injury, Hoechst 33,342 staining and Annexin V-PI double staining were used. As shown in Fig. 3A, treatment with 100 μmol/L 6-OHDA for 24 h, the blue fluorescence intensity of PC12 cells increased, which meant DNA condensation and nuclear fragmentation were occurring, while pretreatment with KuA (5, 10, and 20 μmol/L) could inhibit these apoptotic characteristics.

Annexin V-PI double staining assay was used to further distinguish the features of apoptotic and necrotic cells in response to 6-OHDA and with or without KuA. As shown in Fig. 3B and C, with 100 μmol/L 6-OHDA for 24 h treatment significantly increased in total apoptotic cells (41.54% ± 2.58%, $P < 0.0001$) and late apoptotic cells (37.27% ± 1.56%, $P < 0.0001$). However, pretreatment with KuA (5, 10, and 20 μmol/L) significantly decreased the cell numbers of total and late apoptosis induced, which were total apoptosis

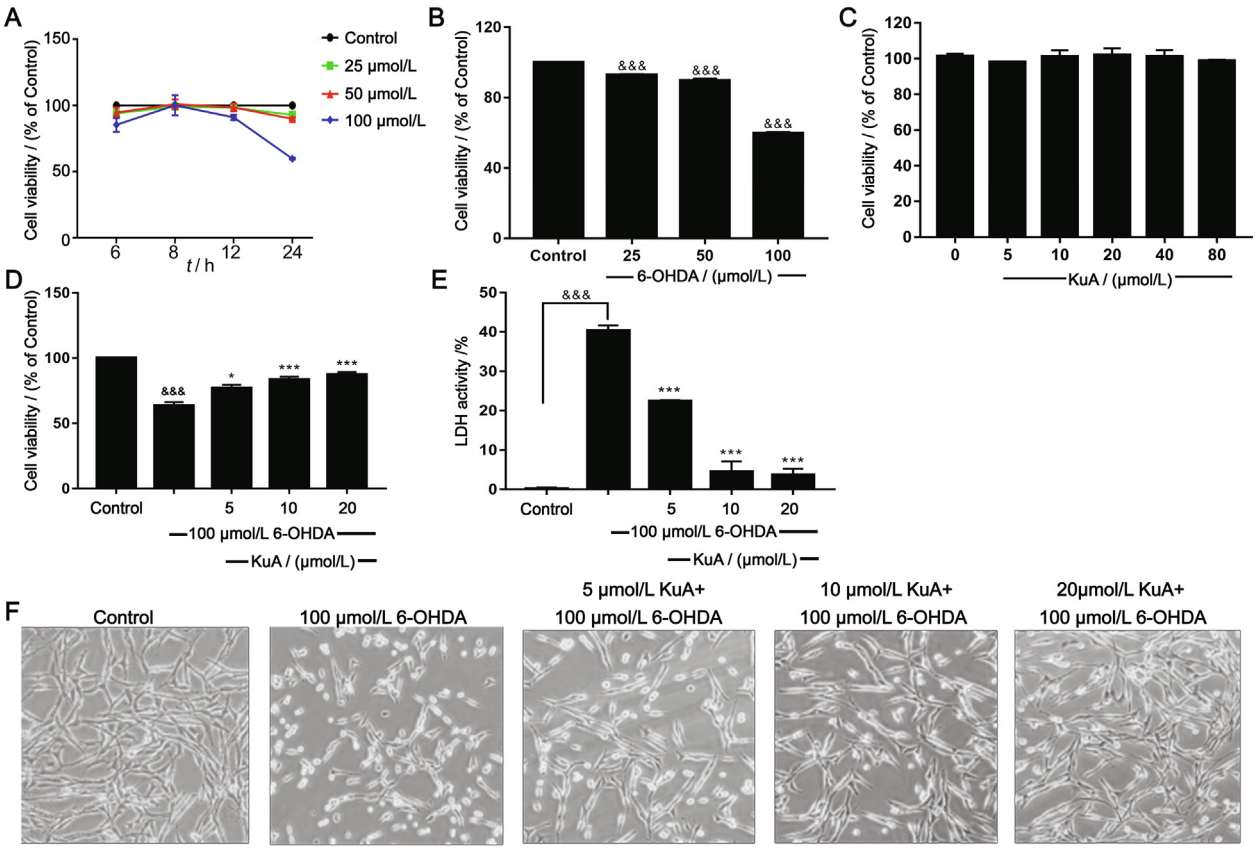

Fig. 2. Neuroprotection of KuA in PC12 cells. (A) Cytotoxic effect of different times of 6-OHDA in PC12 cells. (B) Cytotoxic effect of different concentrations of 6-OHDA in PC12 cells. (C) KuA (5–80 μmol/L) treated alone has no effect on cell viability. (D) Dose-dependent protective effect of pretreatment with KuA against 6-OHDA-induced cytotoxicity in PC12 cells. (E) Morphology of PC12 cells followed by above treatments with an inverted microscope (200 ×). (F) Protective effect of plasma membrane damage determined by LDH release. The data were represented as mean ± S.E.M. ($n = 3$). $^{\&}P < 0.05$, $^{\&\&}P < 0.01$, $^{\&\&\&}P < 0.001$ *vs* control group; $^{*}P < 0.05$, $^{**}P < 0.01$, $^{***}P < 0.001$ *vs* 6-OHDA-treated group.

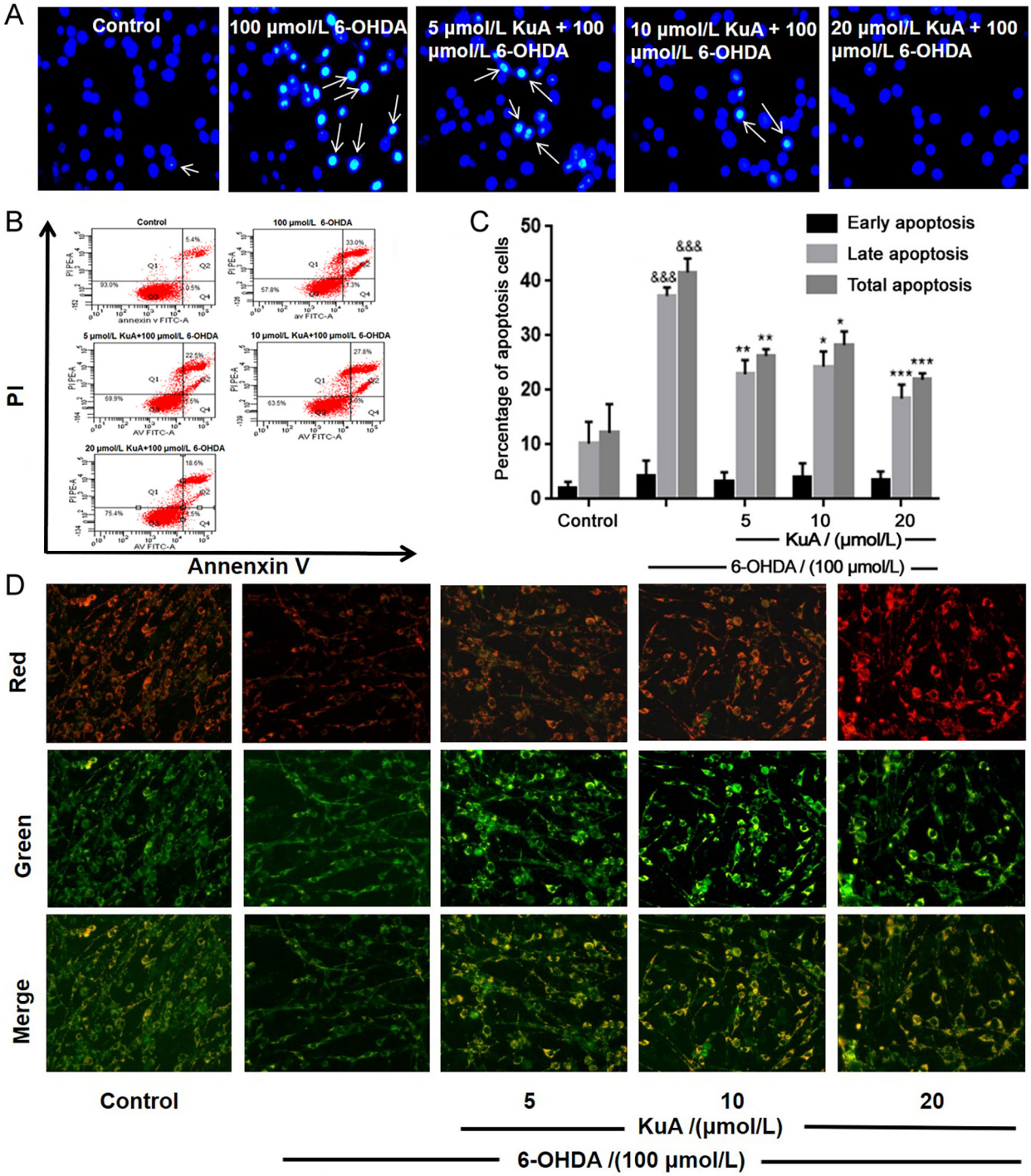

Fig. 3. Effects of KuA on 6-OHDA-induced apoptosis and MMP change in PC12 cells. (A) Morphological changes of nuclear chromatin by Hoechst 33,342 staining were observed using a fluorescence microscope (200 ×). (B) Distribution of viable (lower left, Annexin V- PI-) necrotic (upper left, Annexin V- PI +) late apoptotic (upper right, Annexin V + PI +) and early apoptotic (lower right, Annexin V + PI-). (C) Quantitative analysis of bar graphs showed percentage of late apoptotic and total apoptotic cells. (D) MMP fluorescence images visualized by a fluorescence microscope (200 ×). Data were represented as mean ± S.E.M. ($n = 3$). $^{\&\&\&}P < 0.001$ *vs* control group; $^{*}P < 0.05$, $^{**}P < 0.01$ and $^{***}P < 0.001$ *vs* 6-OHDA-treated group.

(26.28% ± 1.25%, $P < 0.01$) and late apoptosis (22.90% ± 2.62%, $P < 0.01$); total apoptosis (28.26% ± 2.49%, $P < 0.05$) and late apoptosis (24.34% ± 2.77%, $P < 0.05$); total apoptosis (21.90% ± 1.15%, $P < 0.001$) and late apoptosis (18.45% ± 2.58%, $P < 0.001$), respectively. These results indicated that KuA could effectively reduce the apoptosis of PC12 cells induced by 6-OHDA, especially the late apoptosis of cells.

3.4. Effects of KuA on mitochondrial membrane potential (MMP)

To characterize the changes in mitochondrial events induced by 6-OHDA and / or KuA treatment, the collapse of MMP in PC12 cells was monitored using the JC-1 staining. As shown in Fig. 3D, the fluorescence intensity of high green and low red (low MMP) was presented in 6-OHDA treated group, while pretreatment with KuA (5,

10, and 20 μmol/L) could decrease the fluorescence intensity of green and increase the fluorescence intensity of red (high MMP). These results indicated that KuA could improve the function of mitochondria.

3.5. KuA attenuated ROS production and MDA level and improved SOD activity in PC12 cells

6-OHDA-treated PC12 cells induce reactive oxygen species (ROS) production and cause oxidative stress injury. Therefore, in order to investigate the effect of KuA on the generation induced by 6-OHDA, the ROS-sensitive fluorescence dye, DCFH-DA was performed by flow cytometry. As shown in Fig. 4A, exposure to 6-OHDA could cause an elevation of the intracellular ROS, which could suppress by KuA pretreatment (5, 10, and 20 μmol/L). The results indicated that KuA had the ability to eliminate 6-OHDA-induced accumulation of intracellular ROS.

Increased ROS levels are known to induce MDA. As shown in Fig. 4B, 6-OHDA significantly increased MDA content (383.34% ± 63.08%) in PC12 cells, which was significantly ameliorated to (202.90% ± 2.89%), (133.82% ± 50.44%) and (82.13% ± 35.86%), respectively by KuA (5, 10, and 20 μmol/LM). SOD could be regarded as an antioxidant defense in response to the oxidative stress. KuA markedly increased SOD activity (90.17% ± 5.54%, 99.77% ± 6.32%, 112.48% ± 4.87%) compared with that in the 6-OHDA treated group (64.43% ± 2.98%), suggesting that KuA could alleviate the oxidative damage induced by 6-OHDA (Fig. 4C).

3.6. KuA restored Bcl-2/Bax ratio, decreased cl-casp-9, cl-casp-3 and cl PARP expression

The mitochondrial apoptosis pathway is mainly involved in the apoptosis of dopaminergic neuronal cells. The results showed that 6-OHDA treatment alone caused a significant increase in the pro-apoptotic proteins Bad, Bax, cytochrome *C*, cleaved Caspase-9, cleaved Caspase-3 and cleaved PARP, as well as a dramatic decrease in the levels of the anti-apoptotic protein Bcl-2, Caspase-9, Caspase-3 and PARP (Fig. 5). However, pretreatment with KuA significantly increased the ratio of Bcl-2/Bax, and the expression of Caspase-9, Caspase-3, and PARP, while suppressed the expression of Bad, cytochrome *C*, cleaved Caspase-9, cleaved Caspase-3, and cleaved PARP in PC12 cells induced by 6-OHDA (Fig. 5). These results suggested that KuA could inhibit the mitochondrial apoptosis to prevent cell injury.

3.7. KuA attenuated iron overload induced by 6-OHDA via chelating iron and alleviating ferrous iron influx

Several lines of evidence showed a rapid accumulation of nigral iron in animals following intoxication with the Parkinsonian agents 6-OHDA (Finkelstein et al., 2017). To measure the content of iron in cytosol, the specific fluorescence probe calcein AM, which binds iron specifically, and iron chelator deferoxamine mesylate (DFO) were used. As shown in Fig. 6A, 10 μmol/L 6-OHDA for 24 h could significantly increase the iron content compared to control group, presumably because of the rapid release of iron from various intracellular sources and the increase of the ferrous iron influx. However, pretreatment with 20 μmol/L KuA could improve the fluorescence intensity compared with 6-OHDA/Fe^{2+} group. Moreover, we investigated the changes of fluorescence intensity to evaluate the effect of KuA on the ferrous iron influx. As shown in Fig. 6B, the fluorescence intensity in the cells was decreased after incubation with 100 μmol/L Fe^{2+} for 30 min, and it was further reduced after pretreatment with 10 μmol/L 6-OHDA for 24 h, while 20 μmol/L KuA could increase the fluorescence intensity, suggesting that KuA could decrease the enhancement of iron uptake induced by 6-OHDA. As shown in Fig. 6C, KuA could significantly increase the fluorecence intensity compared with the Fe^{2+} group, demonstrating that KuA may be the potential iron chelator.

3.8. Regulation of KuA on expression of iron-related proteins with 6-OHDA treatment

To clarify the mechnisms of KuA in regulating intracellular iron homeostasis and the consequent neuroprotective roles in neuronal cells, the iron proteins involving in iron uptake (DMT1, TfR), transport (ferroportin and hephaestin), and storage (Ferritin) were studied with the treatment of 6-OHDA. As shown in Fig. 7A, 6-OHDA elevated the levels of DMT1 and TfR, indicating 6-OHDA increase the iron influx, which could downregulate after pretreatment with KuA. Meanwhile, expression of ferroportin and hephaestin, responsible for the iron exportation from cells, was decreased in 6-OHDA treatment, indicating that iron release in those cells may be reduced, which were reversed by pretreatment with KuA

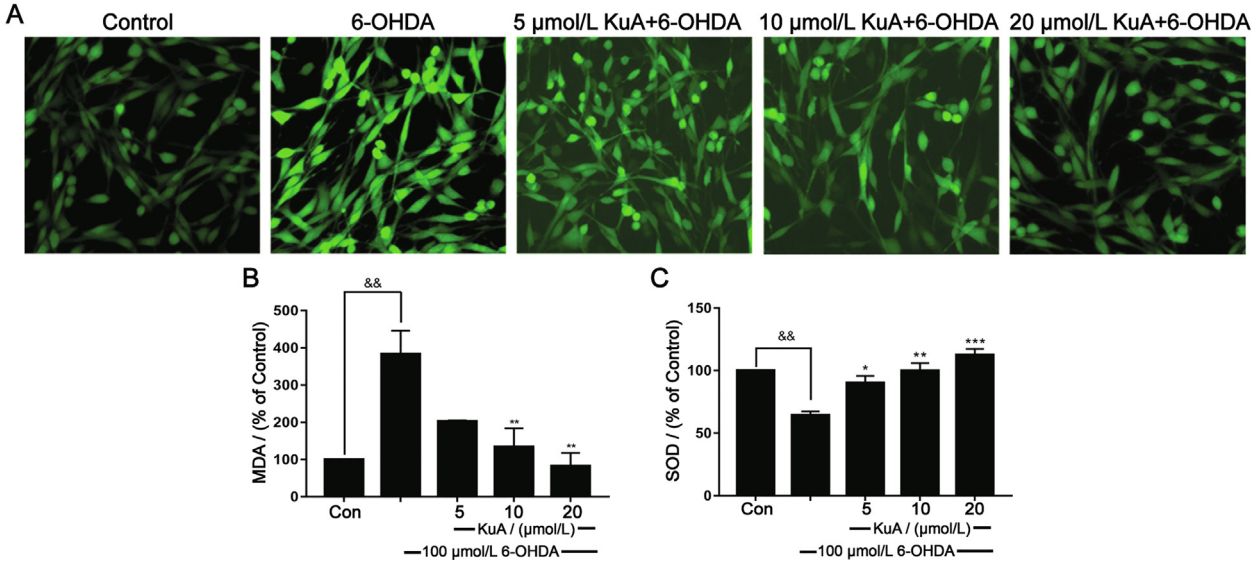

Fig. 4. Neuroprotection of MDCQA on attenuating ROS generation (A), decreased MDA level (B), and improved SOD activities (C) in PC12 cells induced by 6-OHDA. Data were showed as mean ± S.E.M. (n = 3). $^{\&\&}P < 0.01$ *vs* control group; $^{*}P < 0.05$, $^{**}P < 0.01$, and $^{***}P < 0.001$ *vs* 6-OHDA-treated group.

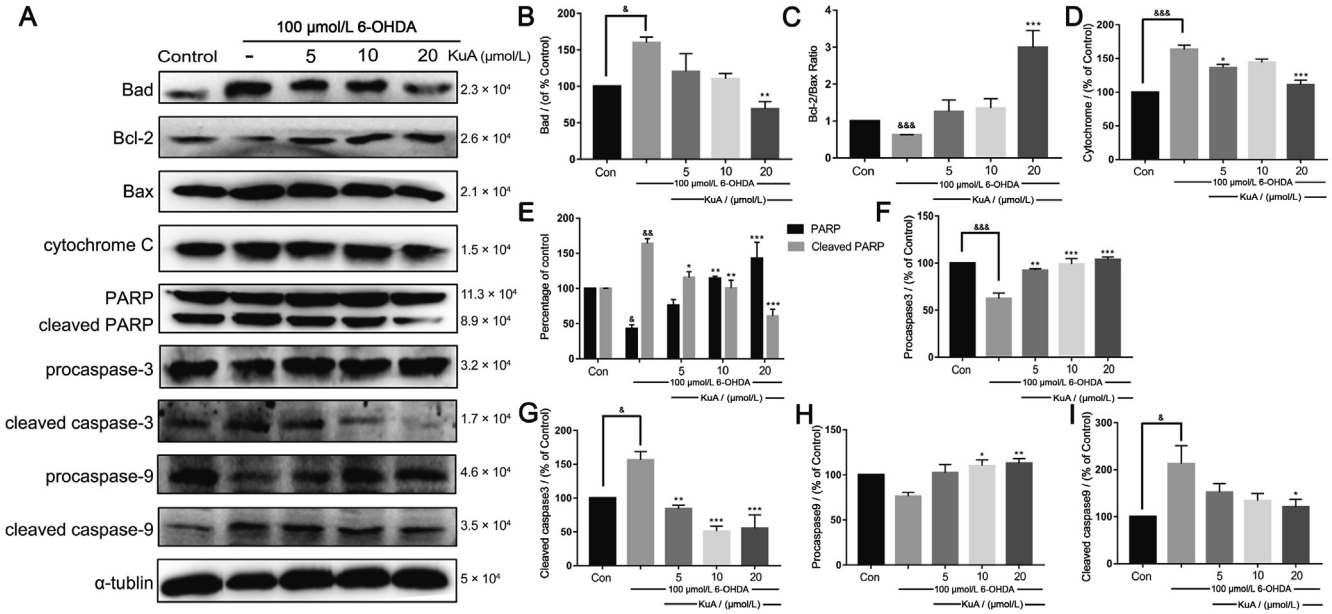

Fig. 5. Neuroprotection of KuA on levels of apoptosis-related proteins in 6-OHDA-treated PC12 cells. (A) Protein expression of Bad, Bax, Bcl-2, cytochrome *C*, PARP and caspase-3/-9. α-tublin and β-actin were used as internal control. (B) - (I) Quantitative analysis of bar graphs showed expressions or ratio of proteins. Data were showed as mean ± S.E.M. (n = 3). $^{\&}P < 0.05$, $^{\&\&}P < 0.01$ and $^{\&\&\&}P < 0.001$ *vs* control group; $^{*}P < 0.05$, $^{**}P < 0.01$, $^{***}P < 0.001$ *vs* 6-OHDA-treated group.

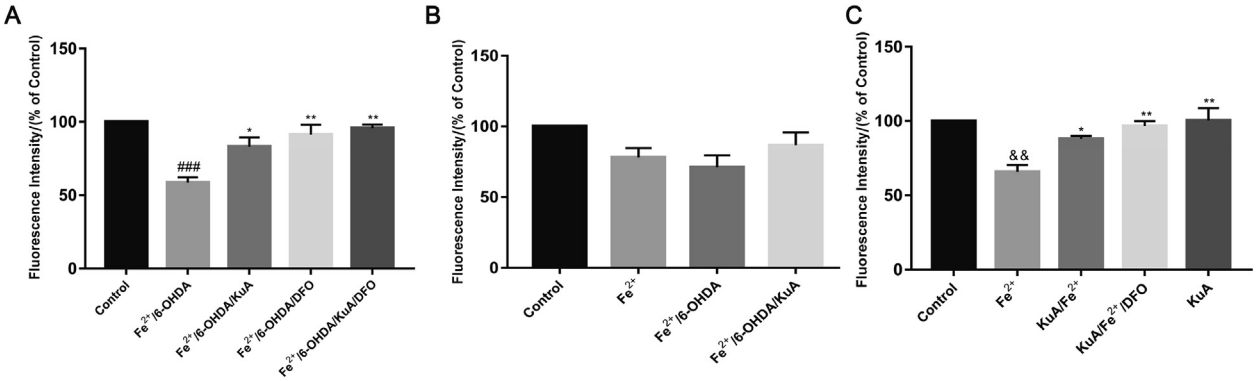

Fig. 6. Iron content (A), iron influx (B) and calcein-indicated iron chelation (C) of KuA in PC12 cells. Cells were pretreated with 20 μmol/L KuA for 4 h, and then treated with 10 μmol/L 6-OHDA for 24 h. After incubation with 1 μmol/L calcein for 30 min, the cells were incubated with 100 μmol/L Fe^{2+} for 30 min, and 50 μmol/L DFO for 30 min lastly. Data were showed as mean ± S.E.M. (n = 3). $^{\&\&}P < 0.01$ and $^{\#\#\#}P < 0.001$ *vs* control group; $^{*}P < 0.05$ and $^{**}P < 0.01$ *vs* Fe^{2+}-treated group and 6-OHDA/Fe^{2+}-treated group.

(Fig. 7B). However, there was an interesting result, which showed a significant up-regulation of Ferritin induced by 6-OHDA, and pretreatment with KuA could down-regulate the expression of Ferritin (Fig. 7C).

3.9. KuA decreased neuron loss and overexpression of α-synuclein in PC12 cells

Tyrosine hydroxylase (TH) is the rate-limiting enzyme responsible for dopamine synthesis, as a specific index of dopamine neurons. Aggregation of α-synuclein was characterized in Parkinson's disease, which was reported that iron deposition and oxidative stress are demonstrated to be involved in the aggregation of α-synuclein (Needham et al., 2018). Hence, the expression of TH and α-synuclein in cytosol were determined by Western blot method. As showed in Fig. 8A, treatment with 6-OHDA for 24 h induced about 50% ($P < 0.05$) loss of TH expression compared to the control group. Pretreatment with KuA (5, 10, and 20 μmol/L) for 4 h could significantly increase the expression of TH by (120.43 ± 2.20)%, (116.01 ± 9.50)%, and (136.45 ± 24.75)%, respectively. Moreover, exposed to 6-OHDA, the expression of α-synuclein in cytosol was significantly increased to 3-fold compared with control group, while the overexpression could be blocked by the pretreatment with KuA (5, 10, and 20 μmol/L) (Fig. 8B). These results suggested that KuA could protect the neuronal cells.

4. Discussion

Several lines of evidence have indicated that there is an accumulation of iron in the neurons of the SN in PD (Zucca et al., 2017), which is a potent generator of free-radicals and causes mitochondrial disfunction (Mastroberardino et al., 2009), as well as accelerates the aggregation of α-synuclein (Kozlowskia et al., 2012). Our previous study demonstrated that KuA could provide neuroprotective effects through mitochondrial pathway, autophagy activation from MPTP/MPP^+ induced Parkinsonian model *in vitro* and *in vivo* (Hu et al., 2017), which reminded that KuA might have anti-PD bioactivity. It is widely accepted that MPP^+ impairs mitochondrial respiration by inhibiting the multi-subunit enzyme complex I of the mitochondrial electron chain that triggers

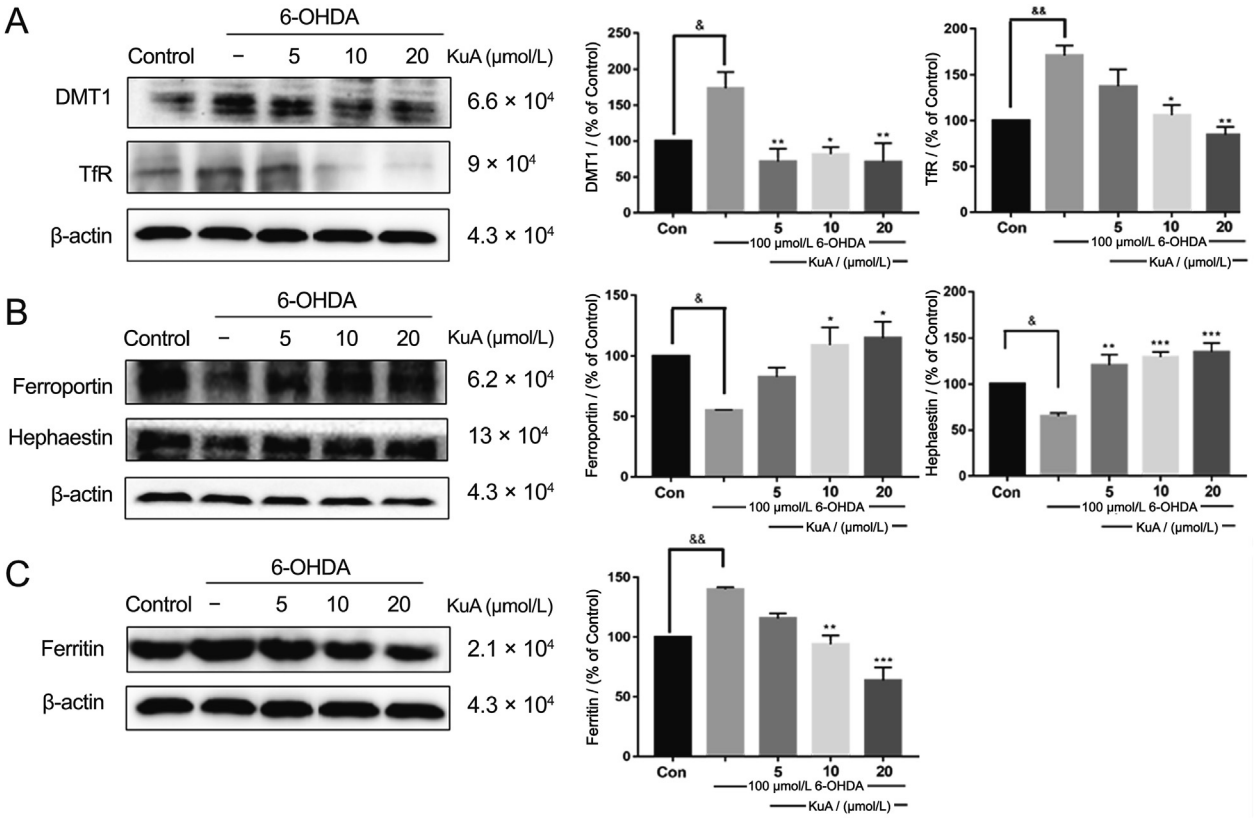

Fig. 7. Regulation of KuA on levels of iron metabolism related proteins in 6-OHDA-treated PC12 cells. (A) Expression of iron transferrin protein: DMT1 and TfR; (B) Expression of iron transfer proteins: ferroportin and hephaestin; (C) Iron storage protein: Ferritin. Data were showed as mean ± S.E.M. (n = 3). $^{\&}P < 0.05$ and $^{\&\&}P < 0.01$ *vs* control group; $^{*}P < 0.05$, $^{**}P < 0.01$, $^{***}P < 0.001$ *vs* 6-OHDA-treated group.

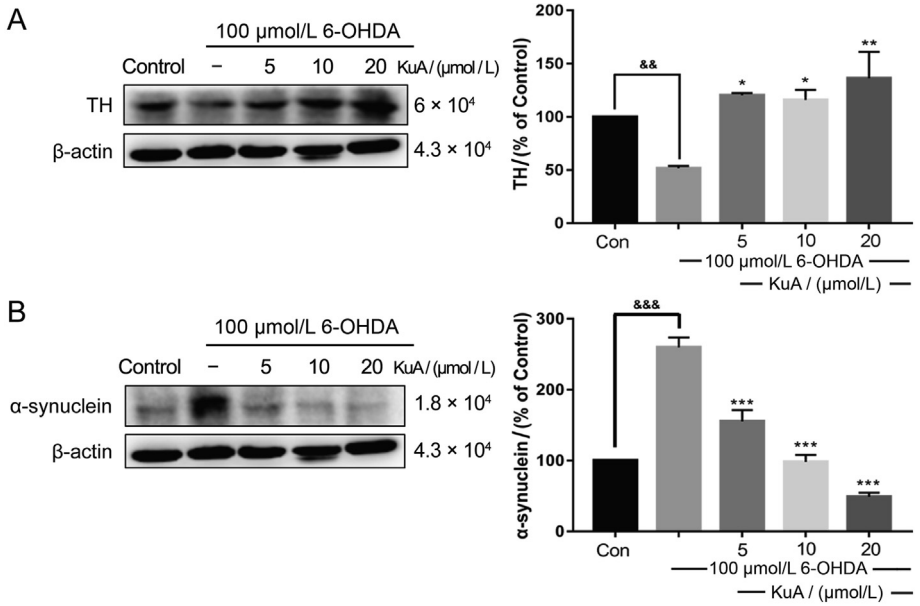

Fig. 8. Neuroprotection of KuA on levels of TH and α-synuclein in 6-OHDA-treated PC12 cells. Levels of (A) TH and (B) α-synuclein proteins were determined by Western blot analysis. β-actin was used as internal control. Data were showed as mean ± S.E.M. (n = 3). $^{\&\&}P < 0.01$ and $^{\&\&\&}P < 0.001$ *vs* control group; $^{*}P < 0.05$, $^{**}P < 0.01$, $^{***}P < 0.001$ *vs* 6-OHDA-treated group.

a transient reduction in midbrain ATP levels and increase of ROS production, whereas, it could not form a classical and stable motor behavior *in vivo* (Bové and Perier, 2012). Moreover, MPTP was harm to laboratory staff, causing neurotoxin in brain after inadvertently smoking. Therefore, we adapted another common Parkinsonian toxin agent, 6-OHDA to further investigate the therapeutic potential of KuA to prevent progressive neurodegeneration in PD.

6-hydroxydopamine (6-OHDA) is a selective neurotoxin that was first reported to cause lesions in nigrostriatal DA neurons in rats (Ungerstedt, 1968). 6-OHDA being hydrophilic cannot cross

the blood brain barrier (BBB), which need to be injected to Substantia Nigra pars Compacta (SNc) and Medial Forebrain Bundle (MFB) causing progressive retrograde DA neuronal degeneration (Jagmag et al., 2016). The neurotoxicity of 6-OHDA occurs through a two-step mechanism involving accumulation of the molecule into catecholaminergic neurons by the DA and noradrenaline membrane transporters, followed by its inhibitory action on mitochondrial complex I (Blum et al., 2001) and the auto-oxidation to form semiquinone and superoxide anions that are subsequently converted to hydroxyl radicals through interaction with H_2O_2 (Yin, Cao, & Xie, 2010). In this study, we found that 100 μmol/L 6-OHDA for 24 h caused about 40% loss of cells (Fig. 2B) and significant increase of LDH release (Fig. 2D) through MTT and LDH assays. LDH is a stable cytoplasmic enzyme that can be found in all cells, which could be another indicator of cell toxicity and could be rapidly released into the extracellular milieu when the plasma membrane is damaged (Ji & Min, 2016). Therefore, LDH is used frequently as a reliable indicator of neuronal plasma membrane damage. The results of our study indicated that pretreatment with different concentrations of KuA markedly attenuated both the decrease in cell viability and the increase in LDH release (Fig. 2C D).

Previous study showed that apoptosis played a vital role in programmed cell death induced by 6-OHDA (Afshin-Majd et al., 2017). We also studied apoptotic cell death in this system, which was typically characterized by cell shrinkage and nuclear condensation. Pretreatment with KuA significantly attenuated these apoptotic features, which was verified by Hoechst and Annexin V-PI staining (Fig. 3). These data proved that KuA had a strong anti-apoptotic effect against 6-OHDA.

Previous study had found that appropriate concentration of 6-OHDA can completely inhibit the activity of NADH dehydrogenase and cytochrome *C* oxidase in the mitochondrial respiratory chain (Höglinger et al., 2003), which could be seen that 6-OHDA can cause mitochondrial respiratory chain block and selective DA neurons toxicity. 6-OHDA selectively enters catecholamine neurons through catecholamine reuptake and reversibly inhibits mitochondrial complex I and complex IV from impairing mitochondrial metabolism, leading to mitochondrial dysfunction and eventually cell death (Henze et al., 2005; Jia et al., 2005). Our experimental result regarding the ability of 6-OHDA decreasing MMP are consistent with previous findings, where showed that KuA effectively attenuated this adverse effect, as seen in Fig. 3D. Therefore, to determine the mechanism by which pretreatment with KuA against 6-OHDA-induced apoptosis, Western blot was used to investigate whether mitochondrion mediated apoptotic pathway involved or not. According to previous reported studies, the Bcl-2 family proteins are involved in the regulation of neuronal apoptotic cell death. The results showed that 6-OHDA significantly decreased Bcl-2/ Bax expression ratio and up-regulated cytochrome *C* in cytosol, which subsequently activated Caspase-9 and Caspase-3 (Fig. 5). However, pretreatment with KuA exerted anti-apoptotic effects against 6-OHDA-induced caspase dependent apoptosis, actually being embodied in the up-regulation of Bcl/ Bax ratio, the down-regulation of cytochrome *C*, PARP, Caspase-9 and Caspase-3 (Fig. 5).

Oxidative stress, a disturbance of the balance between the antioxidant defense system and the generation of ROS, is closely associated with the dopaminergic neurodegenerative process of PD (Cui et al., 2016). MDA, a byproduct of lipid peroxidation, is produced under conditions of oxidative stress, which reflects the oxidative injury of plasma membrane, and the resulting thiobarbituric acid reactive substances are associated with oxidant stress and lipid peroxidation (Xiao et al., 2008). In the contrast, an important antioxidant enzyme, called SOD has been indicated to directly catalyze the transformation of peroxides and superoxides to nontoxic species (Jin, Liu, Jia, Li, & Wang, 2015). Therefore, we tested the levels of intercellular ROS production, MDA content, and SOD activity after treated with 6-OHDA, results showed that 6-OHDA could induce cell oxidative injury and pretreated with KuA can attenuate these changes, appearing on the decrease of ROS and MDA production and increase of SOD activity (Fig. 4).

The PC12 cell line belongs to an adrenergic neural tumor pheochromocytoma cell line and has the ability to proliferate and differentiate, implying that this cell line is different from mature neurons in some aspects of cell metabolism, such as iron needs (Zhang, Song, Jiang, Bi, & Xie, 2014). Iron is essential for many cellular functions, including energy production, DNA synthesis and repair, phospholipid metabolism, myelination and neurotransmitter synthesis (Dusek et al., 2016). A significant body of evidence from post mortem PD brain studies point to ongoing iron dependent oxidative stress may be involved in the pathology of nigrostriatal dopamine neuron degeneration, which also occurs in the substantia nigra pars compacta of rats and monkeys exposed by 6-OHDA (Shachar et al., 2004; Ganguly et al., 2020). Studies have demonstrated that intraventricular pre-injection of desferral (a selective iron chelator) in rats attenuates 6-OHDA-induced lesions of nigrostriatal dopamine neurons (Linert et al., 1996; Zhao, 2019). From the chemical structure, KuA is a linear spermine alkaloid with a large molecule flexibility and two adjacent phenolic hydroxyl groups (Fig. 1), which indicates KuA may have ability of iron chelation. As expected, KuA exhibited some iron chelation ability (Fig. 6C), as well as the decrease of iron accumulation induced by 6-OHDA (Fig. 6A). These results suggested that KuA may be a potential iron chelator, which protected neurons from iron deposition induced by 6-OHDA.

Neuronal iron homeostasis is maintained by regulation of intracellular iron uptake, transport, and storage, because high iron levels can be detrimental to brain function (Rhodes & Ritz, 2008). Accordingly, Fe influx involves transferrin (Tf)-bound Fe uptake and the influx transporter DMT1. DMT1 is one of the proteins responsible for cell iron uptake, which can be upregulated by 6-OHDA, resulting in excess iron influx and neurodegeneration (Chen, Kanthasamy, & Reddy, 2015). In our study, we also found that 6-OHDA increased the expression of DMT1 and TfR, which directly caused the increase of iron influx (Fig. 6B and 7A), while could significantly inhibited by KuA. Ferroportin and hephaestin are proteins that responsible for the iron exportation from cells and furthermore, ferroportin1 is the only known mammalian cellular iron exporter, facilitating iron export process in the presence of hephaestin (Wang, Bi, & Xie, 2015). In our study, we found that KuA could upregulate the expression of ferroportin1 and hephaestin and, in turn, facilitate iron export and decrease cellular iron content (Fig. 6C and 7B). It has been reported that 6-OHDA could release iron from ferritin and subsequently increase iron content (Chen, Kanthasamy, & Reddy, 2015). Interestingly, it was noticed that 6-OHDA significantly increased the expression of Ferritin (Fig. 7C), which meant iron storage was increased, and iron content was decreased. We supposed that 6-OHDA induced a sharp increase on iron content, causing a cell stress response, leading to the upregulation of ferritin. Meanwhile, KuA could downregulate the expression of DMT1 and TfR, upregulate the expression of ferroportin1 and Hephaestin, and in turn, decrease the cellular iron content, which did not cause the occurrence of cell stress response and overexpression of Ferritin induced by 6-OHDA.

Accordingly, brain regions that have a high burden of iron accumulation are likely to be more susceptible to oxidative stress. The situation is further aggravated in DA neurons as iron can promote the oxidation of dopamine and facilitate the formation of dopamine quinone as well as the neurotoxic 6-OHDA (Hare and Double, 2016), which could show a significantly TH^+ cell loss. It has been reported that the binding of Fe (III) with α-synuclein accelerated the amyloid formation of α-synuclein, which is

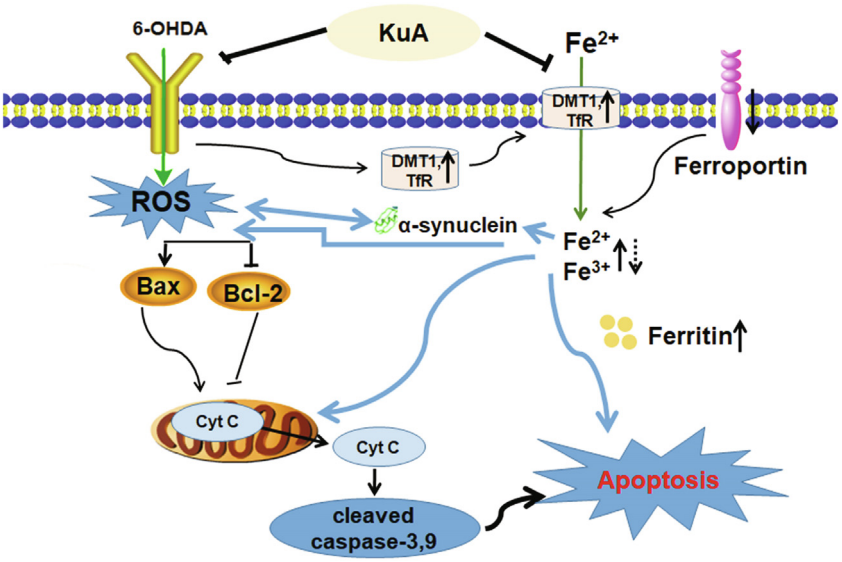

Fig. 9. Mechanism of KuA against 6-OHDA-induced PC12 cells injury.

particularly toxic to DA neurons. In our study, we found KuA could decrease the overexpression of α-synuclein and increase the expression of TH, preventing neuron loss from 6-OHDA exposure (Fig. 8).

5. Conclusion

In summary, it was the first time that we found that KuA may be a potential iron chelator. In addition, our results suggested that KuA protected against 6-OHDA-induced injury in PC12 cells through direct chelating cellular iron, inhibiting iron overload, scavenging of intracellular ROS induced by 6-OHDA and blocking classic mitochondrial apoptotic pathway as well as maintaining iron homeostasis (Fig. 9). Thus, KuA is potentially a novel therapeutic compound for the treatment of early PD.

Declaration of Competing Interest

Neither any of the authors have anything to disclose regarding this manuscript nor do they have any potential conflicts of interest to report concerning this article.

Acknowledgment

This work was supported by the Natural Science Foundation of Liaoning Province, China. (Project number: 20170540945).

Appendix A. Supplementary data

Supplementary data to this article can be found online at https://doi.org/10.1016/j.chmed.2020.12.004.

References

Afshin-Majd, S., Bashiri, K., Kiasalari, Z., Baluchnejadmojarad, T., Sedaghat, R., & Roghani, M. (2017). Acetyl- l -carnitine protects dopaminergic nigrostriatal pathway in 6-hydroxydopamine-induced model of Parkinson's disease in the rat. *Biomedicine & Pharmacotherapy, 89*, 1–9.

Blum, D., Torch, S., Lambeng, N., Nissou, M.-F., Benabid, A.-L., Sadoul, R., & Verna, J.-M. (2001). Molecular pathways involved in the neurotoxicity of 6-OHDA, dopamine and MPTP: Contribution to the apoptotic theory in Parkinson's disease. *Progress in Neurobiology, 65*(2), 135–172.

Bové, J., & Perier, C. (2012). Neurotoxin-based models of Parkinson's disease. *Neuroscience, 211*, 51–76.

Cui, C., Cui, N., Wang, P., Song, S., Liang, H., & Ji, A. (2016). Neuroprotective effect of sulfated polysaccharide isolated from sea cucumber Stichopus japonicus on 6-OHDA-induced death in SH-SY5Y through inhibition of MAPK and NF-κB and activation of PI3K/Akt signaling pathways. *Biochemical and Biophysical Research Communications, 470*(2), 375–383.

Chen, D., Kanthasamy, A. G., & Reddy, M. B. (2015). EGCG protects against 6-OHDA-induced neurotoxicity in a cell culture model. *Parkinson's Disease, 2015*, 1–10.

Devos, D., Moreau, C., Devedjian, J. C., Kluza, J., Petrault, M., Laloux, C., & Bordet, R. (2014). Targeting chelatable iron as a therapeutic modality in Parkinson's disease. *Antioxidants & Redox Signaling, 21*(2), 195–210.

Dusek, P., Schneider, S. A., & Aaseth, J. (2016). Iron chelation in the treatment of neurodegenerative diseases. *Journal of Trace Elements in Medicine and Biology, 38*, 81–92.

Finkelstein, D. I., Billings, J. L., Adlard, P. A., Ayton, S., Sedjahtera, A., Masters, C. L., Wilkins, S., Shackleford, D. M., Charman, S. A., Bal, W., Zawisza, I. A., Kurowska, E., Gundlach, A. L., Ma, S., Bush, A. I., Hare, D. J., Doble, P. A., Crawford, S., Gautier, E. CL., Parsons, J., Huggins, P., Barnham, K. J., & Cherny, R. A. (2017). The novel compound PBT434 prevents iron mediated neurodegeneration and alpha-synuclein toxicity in multiple models of Parkinson's disease. *acta neuropathol commun, 5*(1).

Funayama, S., Yoshida, K., Konno, C., & Hikino, H. (1980). Structure of kukoamine A, a hypotensive principle of Lycium chinense root barks1. *Tetrahedron Letters, 21*(14), 1355–1356.

Hare, D. J., & Double, K. L. (2016). Iron and dopamine: A toxic couple. *Brain, 139*(4), 1026–1035.

Henze, C., Earl, C., Sautter, J., Schmidt, N., Themann, C., Hartmann, A., & Oertel, W. H. (2005). Reactive oxidative and nitrogen species in the nigrostriatal system following striatal 6-hydroxydopamine lesion in rats. *Brain Research, 1052*(1), 97–104.

Höglinger, G.U., Géraldine, C., Michel, P.P, Medja, F., Anne, L., & Ruberg M. (2003). Dysfunction of mitochondrial complex I and the proteasome: interactions between two biochemical deficits in a cellular model of Parkinson's Disease. Journal of Neurochemistry, 86(5), 1297-1307.

Hu, X. L., Gao, L. Y., Niu, Y. X., Tian, X., Wang, J., Meng, W. H., & Zhao, Q. C. (2015). Neuroprotection by Kukoamine A against oxidative stress may involve N-methyl-d-aspartate receptors. *Biochimica et Biophysica Acta (BBA) - General Subjects, 1850*(2), 287–298.

Hu, XiaoLong, Song, Q. I., Li, X., Li, D. D., Zhang, Q., Meng, W. H., & Zhao, Q. C. (2017). Neuroprotective effects of Kukoamine A on neurotoxin-induced Parkinson's model through apoptosis inhibition and autophagy enhancement. *Neuropharmacology, 117*, 352–363.

Jagmag, S. A., Naveen, T., Shukla, S. D., Sankar, M., & Sukant, K. (2016). Evaluation of models of parkinson's disease. *Frontiers in Neuroscience, 9*(92), 503.

Jia, R., Gou, Y., Ho, L., Ng, C., Tan, N., & Chan, H. (2005). Anti-apoptotic activity of Bak Foong Pills and its ingredients on 6-hydroxydopamine-induced neurotoxicity in PC12 cells. *Cell Biology International, 29*(10), 835–842.

Jia, W., Xu, H., Du, X., Jiang, H., & Xie, J. (2015). Ndfip1 attenuated 6-OHDA–induced iron accumulation via regulating the degradation of DMT1. *Neurobiology of Aging, 36*(2), 1183–1193.

Jin, X., Liu, Q., Jia, L., Li, M., & Wang, X. (2015). Pinocembrin attenuates 6-OHDA-induced neuronal cell death through Nrf2/ARE pathway in SH-SY5Y cells. *Cellular and Molecular Neurobiology, 35*(3), 323–333.

Ji, T., & Min, K. (2016). Neuroprotective effects of biochanin against β-amyloid-induced neurotoxicity in PC12 cells via a mitochondrial-dependent apoptosis pathway. *Molecules:basel, Switzerland, 21*(5), 548.

Jomova, K., Vondrakova, D., Lawson, M., & Valko, M. (2010). Metals, oxidative stress and neurodegenerative disorders. *Molecular and Cellular Biochemistry, 345*(1-2), 91–104.

Jung, S., Chung, Y., & Oh, Y. J. (2017). Breaking down autophagy and the ubiquitin proteasome system. *Parkinsonism & Related Disorders, 46*.

Kozlowski, H., Luczkowski, M., Remelli, M., & Valensin, D. (2012). Copper, zinc and iron in neurodegenerative diseases (Alzheimer's, Parkinson's and prion diseases). *Coordination Chemistry Reviews, 256*(19-20), 2129–2141.

Linert, W., Herlinger, E., Jameson, R. F., Kienzl, E., Jellinger, K., & Youdim, M. B. H. (1996). Dopamine, 6-hydroxydopamine, iron, and dioxygen — their mutual interactions and possible implication in the development of Parkinson's disease. *Biochimica et Biophysica Acta (BBA) - Molecular Basis of Disease, 1316*(3), 160–168.

Liu, J., Jiang, X., Zhang, Q., Lin, S., Zhu, J., Zhang, Y., Du, J., Hu, X., Meng, W., & Zhao, Q. (2017). Neuroprotective effects of Kukoamine A against cerebral ischemia via antioxidant and inactivation of apoptosis pathway. *Neurochemistry International, 107*, 191–197.

Luo, L., Chen, J., Su, D., Chen, M., Luo, B., Pi, R., & Wang, R. (2017). L-F001, a multifunction ROCK inhibitor prevents 6-OHDA induced cell death through activating Akt/GSK-3beta and Nrf2/HO-1 signaling pathway in PC12 cells and attenuates MPTP-induced dopamine neuron toxicity in mice. *Neurochemical Research, 42*(2), 615–624.

Needham, L. M., Weber, J., Fyfe, J. W. B., Kabia, O. M., Do, D. T., Klimont, E., & Lee, S. F. (2018). Bifunctional fluorescent probes for detection of amyloid aggregates and reactive oxygen species. *Royal Society Open Science, 5*(2), 171399.

Mastroberardino, P. G., Hoffman, E. K., Horowitz, M. P., Betarbet, R., Taylor, G., Cheng, D., Na, H. M., Gutekunst, C.-A., Gearing, M., Trojanowski, J. Q., Anderson, M., Chu, C. T., Peng, J., & Greenamyre, J. T. (2009). A novel transferrin/TfR2-mediated mitochondrial iron transport system is disrupted in Parkinson's disease. *Neurobiology of Disease, 34*(3), 417–431.

Piletska, E. V., Burns, R., Terry, L. A., & Piletsky, S. A. (2012). Application of a molecularly imprinted polymer for the extraction of kukoamine A from potato peels. *Journal of Agriculture and Food Chemistry, 60*(1), 95–99.

Rhodes, S. L., & Ritz, B. (2008). Genetics of iron regulation and the possible role of iron in Parkinson's disease. *Neurobiology of Disease, 32*(2), 183–195.

Shachar, D. B., Kahana, N., Kampel, V., Warshawsky, A., & Youdim, M. B. H. (2004). Neuroprotection by a novel brain permeable iron chelator, VK-28, against 6-hydroxydopamine lession in rats. *Neuropharmacology, 46*(2), 254–263.

Ungerstedt, U. (1968). 6-hydroxy-dopamine induced degeneration of central monoamine neurons. *European Journal of Pharmacology, 5*(1), 107–110.

Upasana, G., Anindita, B., Sankha, S. C., Upinder, K., Oishimaya, S., Roberto, C., & Sasanka, C. (2020). Interaction of α-synuclein and Parkin in iron toxicity on SH-SY5Y cells: Implications in the pathogenesis of Parkinson's disease. Biochemical Journal, 477(6), 1109-1122

Vassis, S., Karigiannis, G., Balayiannis, G., Militsopoulou, M., Mamos, P., Francis, G. W., & Papaioannou, D. (2001). Simple syntheses of N-alkylated spermidine fragments and analogues of the spermine alkaloid kukoamine A. *Tetrahedron Letters, 42*(8), 1579–1582.

Wang, J., Bi, M., & Xie, J. (2015). Ceruloplasmin is Involved in the nigral iron accumulation of 6-OHDA-lesioned rats. *Cellular and Molecular Neurobiology, 35*(5), 661–668.

Xiao, X., Liu, J., Hu, J., Zhu, X., Yang, H., Wang, C., & Zhang, Y. (2008). Protective effects of protopine on hydrogen peroxide-induced oxidative injury of PC12 cells via Ca2+ antagonism and antioxidant mechanisms. *European Journal of Pharmacology, 591*(1-3), 21–27.

Xu, H., Jiang, H., Wang, J., & Xie, J. (2010). Rg1 protects the mpp+-treated mes23.5 cells via attenuating dmt1 up-regulation and cellular iron uptake. *Neuropharmacology, 58*(2), 488–494.

Yin, L. L., Cao, Y., & Xie, K. Q. (2010). Decreased RGS9 protein level in the striatum of rodents undergoing MPTP or 6-OHDA neurotoxicity. *Neuroscience Letters, 479*(3), 231–235.

Zhang, H. Y., Song, N., Jiang, H., Bi, M. X., & Xie, J. X. (2014). Brain-derived neurotrophic factor and glial cell line-derived neurotrophic factor inhibit ferrous iron influx via divalent metal transporter 1 and iron regulatory protein 1 regulation in ventral mesencephalic neurons. *Biochimica et Biophysica Acta (BBA) - Molecular Cell Research, 1843*(12), 2967–2975.

Zhang, Y., Cheng, Z., Wang, C., Ma, H., Meng, W., & Zhao, Q. (2016a). Neuroprotective effects of kukoamine a against radiation-induced rat brain injury through inhibition of oxidative stress and neuronal apoptosis. *Neurochemical Research, 41*(10), 2549–2558.

Zhang, Y., Gao, L., Cheng, Z., Cai, J., Niu, Y., Meng, W., & Zhao, Q. (2016b). Kukoamine A Prevents Radiation-Induced Neuroinflammation and Preserves Hippocampal Neurogenesis in Rats by Inhibiting Activation of NF-κB and AP-1. *Neurotoxicity Research, 31*(2), 259–268.

Zhang, Z., Hou, L., Li, X., Ju, C., Zhang, J., Li, X., Wang, X., Liu, C., Lv, Y., & Wang, Y. (2016c). Neuroprotection of inositol hexaphosphate and changes of mitochondrion mediated apoptotic pathway and α-synuclein aggregation in 6-OHDA induced parkinson׳s disease cell model. *Brain Research, 1633*, 87–95.

Zhao, Z. (2019). Iron and oxidizing species in oxidative stress and Alzheimer's disease. *Aging Medicine, 2*(2), 82–87. https://doi.org/10.1002/agm2.12074.

Zhou, F., Chen, Y., Fan, G., Feng, C., Du, G., Zhu, G., Li, Y., Jiao, H., Guan, L., & Wang, Z. (2014). Lead-induced iron overload and attenuated effects of ferroportin 1 overexpression in PC12 cells. *Toxicology in Vitro, 28*(8), 1339–1348.

Zucca, F. A., Segura-Aguilar, J., Ferrari, E., Muñoz, P., Paris, I., Sulzer, D., Sarna, T., Casella, L., & Zecca, L. (2017). Interactions of iron, dopamine and neuromelanin pathways in brain aging and Parkinson's disease. *Progress in Neurobiology, 155*, 96–119.